Earth Materials at the Molecular Level

Martin Kunz*[a], Ronald Miletich, Alexandra Friedrich, and Stephanie Rath

Abstract: The extension of crystallographic methods to minerals at non-ambient conditions and materials of technical interest is of importance for understanding the mutual relationship between crystal structure and physico-chemical properties. We apply this approach to understand the physics of the interior of the Earth as well as to contribute to the search for efficient non-linear optical materials.

Keywords: Materials science · Mineral physics · Mineralogy · Non-ambient conditions

1. Mineralogical Crystallography: Between Earth- and Materials Sciences

A large number of original developments and applications in crystallography have emerged from the earth sciences and inorganic solid-state chemistry. However, this branch is now often regarded as old-fashioned and lacking scientific perspective. One reason for this perception comes from the availability of modern diffractometers, which allows crystal structures of inorganic materials with small to moderate unit-cells to be solved (semi-)automatically without much scientific input. This is in sharp contrast to the scientific challenges posed by the quest to structurally characterize bio-materials or even non-periodic material in the solid state. The notion of mineralogical crystallography as an outdated science is additionally supported by the simple fact that the number of different earth materials is finite and countable and most of the geologically relevant material has been

Correspondence: Prof. Dr. M. Kunz[a]
Laboratory of Crystallography
ETH Zürich
CH–8092 Zürich
Tel.: +411 632 6650
Fax: +411 632 1133
E-Mail: kunz@kristall.erdw.ethz.ch
http://www.kristall.ethz.ch/LFK/
[a]Present address:
Naturhistorisches Museum
Augustinergasse 2
CH–4051 Basel
Tel.: +41 61 266 55 90
Fax: +41 61 266 55 46
E-Mail: martin.kunz@bs.ch

crystallographically described over the past 25 years. This, however, applies only to material under ambient conditions. The ultimate quest of doing crystallography on inorganic materials, however, is to work towards a universal model relating chemical composition, crystallographic structure and physical properties. The benefits of such a model are obvious: In materials science it would be an important step towards tailoring technical materials according to their desired properties. In earth sciences, it would allow to develop a much better mineralogical and physical model of the interior of planets, which is not directly accessible with crystallographic experiments. The pressure in the interior of Jupiter, for example, exceeds 4000 GPa, which is out of experimental range for the foreseeable future.

A promising approach to understand the interdependence between crystal structure and physical properties is to vary the external conditions (temperature, pressure, electric field, magnetic field) and to study the changes of structure and physical properties as a function of external conditions. Correlating the change of structural geometry (interatomic distances and angles, vibrational properties) as well as topology (structural rearrangement) with changing physical properties (thermal expansion, compression, dielectric and magnetic constants) provides crucial information on the relationship between structure and physical properties. Thus, from this point of view, our current crystallographic knowledge on earth materials, which is mainly based on experiments at ambient conditions, is merely a scratch on the surface.

Inorganic material – and minerals in particular – represent ideal systems to establish theoretical models. This is due to three principle reasons: Firstly, the chemical variability of many minerals allows isomorphic chemical substitution. This enables an easy control of the chemical factor. Secondly, the relatively small unit cells and thus number of atoms per unit cell permits high-level computational modeling. This gives us the possibility to test immediately theoretical models on the interdependence of physical properties and structure. A third factor, which should not be underestimated, is the ingenuity of nature to come up with variations and possibilities which a synthetic chemist might never think of. The crystallographic study of minerals can thus provide useful insights into possible pathways for technically interesting material.

The performance of *in situ* studies of earth materials at non-ambient conditions is in many aspects still in its infancy. This means that most of the ancillary equipment necessary to create the non-ambient conditions is not commercially available and still needs to be developed. In the second section, we will give a short overview on our work in this domain. As mentioned above, mineralogical crystallography is in many respects situated somewhere between earth science and materials science. The third section will give an insight in some of our crystallographic contributions to understanding the cycle of water within the earth. The last section will finally focus on an aspect of materials science, namely a crystal chemical approach to understanding inorganic non-linear optical material of the $ABOCO_4$-type (*e.g.* KTP).

2. New Experimental Developments

For earth materials, temperature and pressure are the most interesting external parameters to vary. The reason for this is the desire to understand the physical and chemical properties of earth materials under the conditions prevailing in the interior of planets. It is therefore not surprising that right from the beginning of X-ray diffractometry, first devices to create conditions of high-pressure and high-temperature were developed [1]. Although most of the technical principles had been demonstrated by the early seventies, further advances in the field of *in situ* crystallography at high-pressure and high-temperature were delayed by the limited photon flux of conventional X-ray and UV generators. The advent of the first dedicated synchrotron sources created a big impact on crystallography under non-ambient conditions. The trillion times $(\sim 10^{12})$ increase in brilliance opened new possibilities for *in situ* studies which in turn created new requirements for experimental equipment. One of the more urgent problems proved to be the need for novel detector systems able to cope with the high photon flux. Only by using adequate detectors can one tap the intrinsic potential of the high X-ray brilliance to record data in short time intervals. This in turn allows for time-resolved experiments on reactions and transitions. The specific requirements on a detector system for high-pressure work are a large two-dimensional detecting surface and rapid cycling times. The first is important not only for rapid single-crystal data collection, but also for accurate powder experiments. Powder samples in a diamond anvil are intrinsically very small. This affects the powder statistics, which itself is a crucial factor for the quality of the data. By using a two-dimensional detector, the pressure range up to which powder diffraction can be done quantitatively is significantly extended [2]. There exist two different strategies for two-dimensional detectors. Image-plates are based on a light-sensitive layer where X-rays create virtual signals, which subsequently can be read out in a quantitative way by exciting it with a laser [3]. Charge-coupled devices (CCDs) in contrast use a phosphorous screen to convert X-rays to light, which is subsequently converted into an electronic signal on a CCD chip. Both methods have their advantages and disadvantages. The greatest plus of image-plate systems is the large size. This is of particular advantage for synchrotron high-pressure powder diffraction, since it allows the signal to (Compton-)background ratio to be increased by moving the detecting plate further away without compromising on resolution in reciprocal space. The most significant disadvantage was the often cumbersome and slow readout procedure (off-line readout) and intrinsic spatial distortion problems [4]. In order to optimize such an image-plate system for synchrotron high-pressure work, a fast on-line image-plate detector has been constructed at the ESRF [3]. In order to obtain a high read-out speed, the read-out laser (frequency-doubled Nd:YAG) is scanned along a line through a rotating polygon-mirror. In order to read line by line, the plate is moved by a respective increment after each line. By carefully fine tuning rotation- and translation speed of the mirror and the plate respectively, a maximal read-out speed of 9 sec for an image-plate of 250 x 305 mm² size has been achieved. The whole system is compact enough to be mounted on a beamline, where it can be controlled and operated remotely, thus providing a very fast two-dimensional online detector. This system enabled the very first Rietveld refinement on data collected *in situ* at pressures and temperatures as high as 94 GPa and 2400 K [5].

Fast data collections and new experimental possibilities as offered by modern radiation sources also create a need for small and versatile diamond-anvil high-pressure cells, capable of attaining the highest possible pressures. As with all successful designs, the principle [6] upon which the gasketed diamond-anvil cell operates is elegantly simple. The sample is placed in a pressure chamber created between the flat parallel faces (culets) of two opposed diamond anvils and the hole penetrating a hardened metal foil (= the gasket). The free volume within this chamber is flooded with a pressure-transmitting medium, which in ideal cases exerts hydrostatic pressure on the sample. Pressure is applied by forcing the diamonds together. The force required is not large for even the highest pressures attainable, and can be achieved through simple mechanisms. A common feature of all diamond-anvil cells now used for X-ray diffraction is that they employ this opposed-anvil geometry. There are significant differences, though, in the mechanisms used for generating the applied force, as well as the orientation of the incident and diffracted X-ray beams with respect to the diamond anvils [7][8]. Two modes of diffraction geometry are available for high-pressure, single-crystal X-ray diffraction experiments. The *transmission mode* is used in most designs of diamond anvil cell. Here the incident X-rays pass through one diamond, the single-crystal, and then the opposing diamond. In other designs, however, a lateral, or *transverse*, geometry is adopted where the incident and diffracted X-rays pass through the same diamond and/or the X-ray translucent gasket. Based on the BGI design [9] a modular diamond-anvil-cell system has been developed [8][10]. This new 'ETH'-DAC (Fig. 1) has been constructed as a modular DAC system with replaceable modules for room temperature and high-temperature application. Simultaneously both the outer dimensions and the weight have been significantly reduced. The improvements in design include a bayonet joint with a flexible spring leaf, which holds the diamond anvils in place and a new mounting bracket for goniometer heads, which allows rapid changes and reproducible alignment of the DAC on the diffractometer. These modifications add useful improvements while maintaining all the criteria for generating large and stable pressures.

The majority of combined high-pressure, high-temperature (HP-HT) structural studies have been conducted using powder-diffraction techniques. This technique avoids the inevitable complications of repositioning of the DAC, which is necessary for single-crystal techniques. In order to undertake more quantitative HP-HT studies, it is vital that the cell is heated during the X-ray diffraction measurements. Perhaps the most convenient means of achieving this is to use resistance heaters, where wire windings are placed externally around the diamond and sample region. The excellent thermal conductivity of both diamond and the gasket metal provide an ideal heat transfer from the external heater(s) to the pressure chamber. With the application of an appropriate electrical current, resistance heaters provide uniform temperatures for long periods, which can be determined easily through a thermocouple, which is directly attached to one of the diamond anvils. These heaters, however, are limited to temperatures not much greater than 1000 °C owing to graphitization of the diamonds at high temperatures. An additional constraint for applying external heating is that above several hundred °C a reducing atmosphere, such as hydrogen–argon, is required to prevent oxidation of the cell components and/or the diamonds. The drive towards further miniaturization has led to other similar
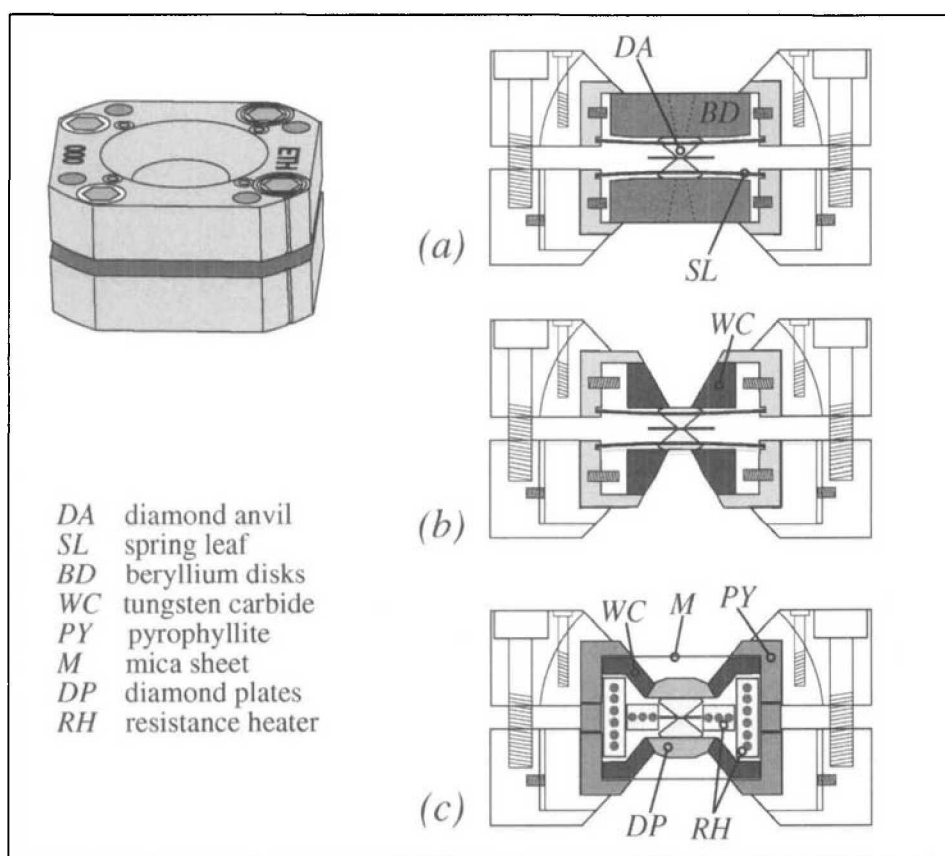
Fig. 1. The modular ETH-DAC system with exchangeable core modules. Cross sections of the DAC with (a) the RT single-crystal module, (b) the HP-HT powder diffraction module, (c) the HP-HT single crystal module.

DA diamond anvil
SL spring leaf
BD beryllium disks
WC tungsten carbide
PY pyrophyllite
M mica sheet
DP diamond plates
RH resistance heater

gasket-based heating systems [11]. In this design the gasket is constructed from a thin layer of electrically insulating alumina sandwiched between two layers of conducting metal. The gasket hole penetrates all three layers and the metal heating wire bridges the conducting steel sheets within the hole. Temperatures in excess of 2000 °C can be achieved with this arrangement. The highest temperatures attained so far in the diamond-anvil cell have been achieved with the use of laser heating [12]. In this technique Nd:YAG or CO_2 laser beams are focused onto the sample, which creates a 10–50 μm hot-spot. Temperatures can exceed 4000 °C [13] with this technique. As the heating is confined almost exclusively to the sample itself, it is not possible to measure the temperature with thermocouples. Optical pyrometric techniques must be employed instead [14]. As expected, the temperature gradients can be extremely large. They can reach up to 400 °C per micron, depending on the temperature at the center of the hot-spot.

The most recent development of a heatable DAC for single-crystal diffraction is that of the modular ETH cell with backing plates made from synthetic diamonds [8][10]. These backing plates are placed onto tungsten carbide seats and,

being transparent, do not require optical access holes. The diamond anvils, the height of which was reduced to 1.2 mm in order to maximize the table-face area, are placed directly onto the diamond discs. The remaining space provides room for two resistive molybdenum-wire heaters embedded in high-temperature ceramic. A thin mica sheet seals the heatable module by covering the conical X-ray window and avoids the outer sides of diamond-backing discs coming into contact with air, thus preventing oxidation of the diamonds. The module itself is thermally insulated by 2 to 3 mm thick pyrophyllite ceramic. The whole cell is placed in a sealed aluminum housing, which allows it to be flooded with a non-oxidizing gas.

3. Water in the Earth's Mantle

A comparison of chemical models of the solar system with the geology of the accessible earth allows us to estimate that about 10% of the earth's water is held in the mantle. The rest is contained in the crust and the oceans. The chemical form and exact distribution of the mantle water is a matter of debate [15] and much effort has gone into unraveling these questions in recent years. The strong interest in this

problem is based in the critical effect that water has on the physical and chemical properties of earth materials. Water affects melting temperatures as well as rheology, viscosity and mechanical strength. Water in the mantle can be present bound in crystal structures as hydroxyl (OH⁻) or be incorporated in the molecular state (H_2O) either as crystal water or dissolved in melts. On the molecular level, the crucial points to understand the effect and relative stability of the various chemical forms of water in the deep earth is the change in the nature of the ubiquitous hydrogen bond as a function of chemical composition, temperature and pressure, respectively. In order to disentangle these various influences on the hydrogen bond, structural studies on simple hydroxides $A(OH)_2$ (A = alkaline-earth metal) have been performed at various pressures and temperatures. The usefulness of this system lies in the fact that alkaline earth metals (Mg^{2+}, Ca^{2+}, Sr^{2+}, Ba^{2+}) have quite similar chemical properties and therefore allow the effects of pressure and temperature on the structure to be isolated. By going from Mg^{2+} to Ba^{2+} along the second main group the size of the metal atom increases without drastically affecting its chemical properties. Increasing ionic radii ('internal' pressure), in turn, simulates to a certain degree 'external' pressure by increasing the cation/anion size ratio [16]. This can therefore be exploited to investigate structural changes at extreme pressures by comparing compounds of identical stoichiometry with similar chemical species but different ionic size at moderate pressures where crystallographic investigations are still possible.

$Mg(OH)_2$ (brucite) and $Ca(OH)_2$ (portlandite) both crystallize at ambient conditions as a layered structure where 50% of the octahedral voids in a hexagonal closest packing (hcp) of oxygen atoms are occupied by the metal cation (Mg, Ca) (Fig. 2). The edge-sharing metal octahedra form layers, which are held together by hydrogen bonds. It is interesting to note that, despite the similar ionic radii of F⁻ (1.30 Å) and OH⁻ (1.34 Å), this structure is distinctly different from those of MgF_2 and CaF_2, which adopt the rutile and fluorite structure, respectively. A first effect of pressure on hydrogen bonds can be seen by either compressing brucite ('external' pressure) or by replacing Mg by Ca and thus using portlandite as a sample ('internal' pressure). In brucite, the O–H bond (~ 0.97 Å) at zero pressure lies on the threefold axis of space-group $P\bar{3}m1$. By this, the hydrogen

atom faces a triangle of oxygen atoms belonging to the adjacent layer. The distances to each of the three oxygen atoms are equivalent by symmetry (~ 2.52 Å). The long O⋯H bond together with an acute O–H⋯O angle (~133°) indicates a fairly weak, trifurcated hydrogen bond. However, as shown by [17] by means of a neutron powder diffraction experiment, this symmetric arrangement is broken upon application of pressure already at 0.4 GPa for deuterated brucite. Instead of a single D-position, three equivalent positions shifted away from the 3-fold axis towards each of the three oxygen atoms are found. It is unclear, however, whether these three positions are dynamically occupied by D or represent a static disorder. Higher pressure might induce a collective freezing or an ordering and thus a decrease of the symmetry from space-group $P\bar{3}ml$ to $C2/m$. Such a decrease in symmetry has not been observed by [17]. Nevertheless, this experimental result suggests that high pressure strengthens the trifurcated hydrogen bond into a single bond with O⋯D of 2.2 Å and O-D⋯O ~ 146°. In slight contrast to this finding, a neutron powder experiment on non-deuterated $Mg(OH)_2$, by [18] found a splitting of the H-position only at a pressure above 10 GPa. Despite the higher pressure for the positional splitting, these authors see indications for an ordering phase transition at elevated pressures, which would be in line with previous spectroscopic studies [19]. The ambiguity on the possible high-pressure phase transition in brucite may be resolved by looking at portlandite. As expected on the basis of the assumption that larger cations can mimic external pressure, portlandite shows already at ambient conditions a splitting of the hydrogen position away from the 3-fold axis [20]. Compression of $Ca(OH)_2$ at RT leads to a reversible amorphization around 6 GPa [21] rather than a symmetry change due to H-ordering. As first observed by Leinenweber [22], this amorphization, however, seems to be caused by a kinetically hindered phase transition. Heating the amorphous material at 6.1 GPa to a temperature of ~ 200 °C promotes a very sharp structural change. This new phase is stable upon cooling, but reverses to portlandite on pressure release. Surprisingly, the structural difference of the new high-pressure phase $(Ca(OH)_2$-II) to portlandite is not mainly found in an ordering or rearrangement of the hydrogen-bonds between the octahedral layers. Instead, it involves a complete rearrangement of the first coordination sphere around the Ca and O at-
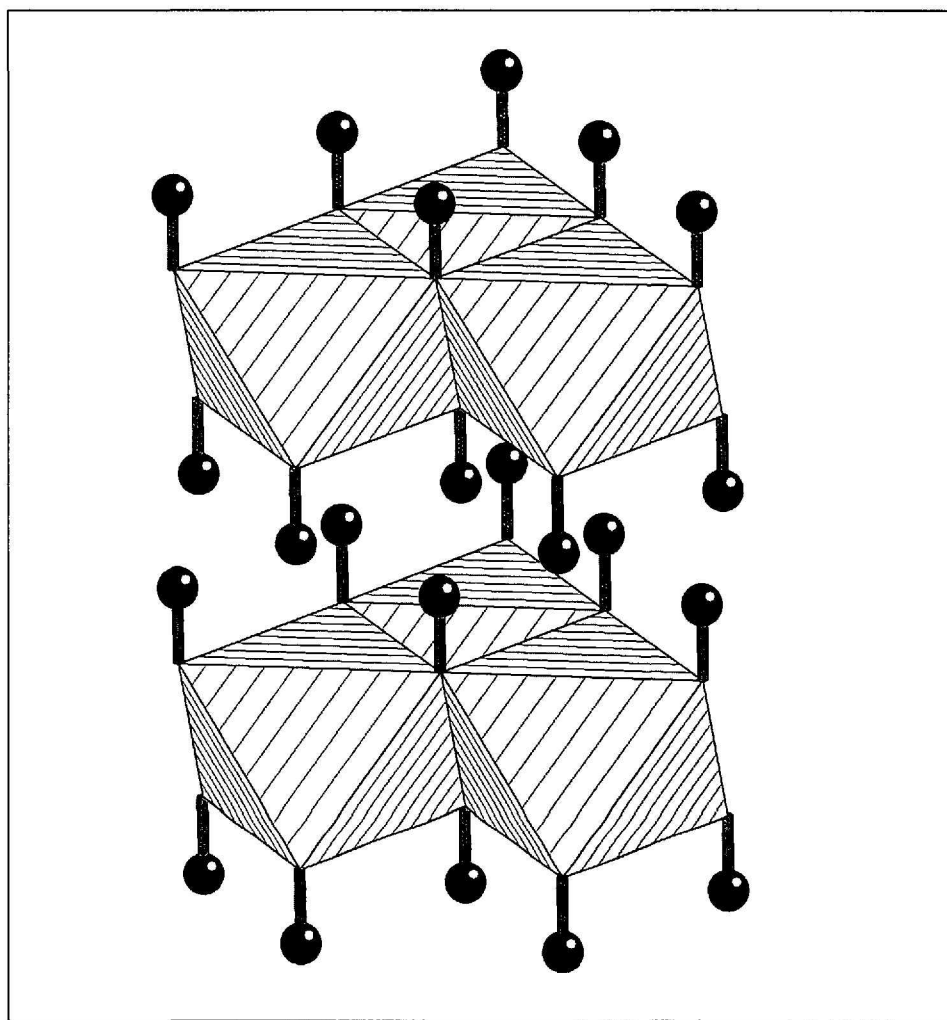

Fig. 2. Polyhedral sketch of the CdI_2 type structure adopted by brucite and portlandite at ambient conditions. Octahedra represent AO_6 coordination octahedra, the small spheres show the hydrogen position. In portlandite, the hydrogen position is split on three positions. Each position is shifted towards one of the three next oxygen atoms of the adjacent layer.
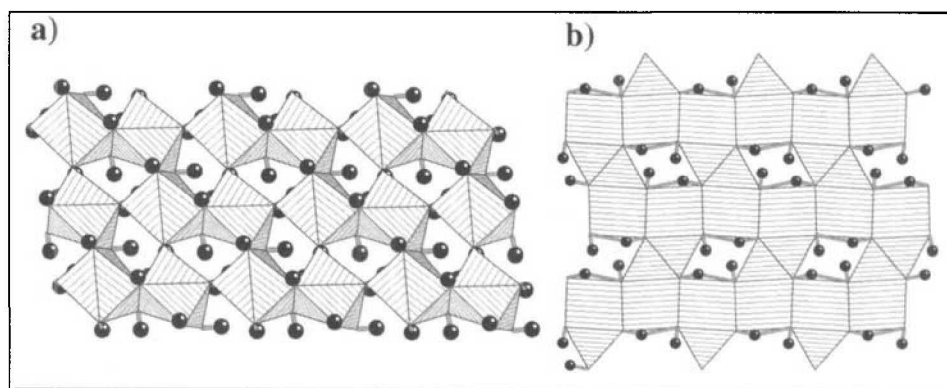

Fig. 3. Comparison of the structures of a) $Ca(OH)_2$-II and b) $Sr(OH)_2$. Although topologically different, both structures are characterized by a 7-fold coordinated metal atom and two 3-, and 4-coordinated oxygen atoms. The MO_7 polyhedra form an edge-linked framework, the hydrogen atoms are situated in the cavities within this structure.

oms. Thus, in the high-pressure form of $Ca(OH)_2$, Ca is not found in 6-fold octahedral coordination but 7-coordination [23]. Furthermore, $Ca(OH)_2$-II forms a three-dimensional network of CaO_7 polyhedra rather than a layered structure like brucite and portlandite. Interesting is also the fact that in the high-pressure phase at

a pressure just above the phase transition, the hydrogen bonds (as deduced from the X-ray data combined with pseudo-potential total energy calculations) seem not to be relaxed (Kunz, Winkler and Papoular, unpublished data). An average O⋯H distance of 1.75 Å and O-H⋯O angle of ~ 164° point to strong hydrogen bonding.

In fact, this hydrogen bonding is even stronger than observed for brucite at 10 GPa [17][18]. Unfortunately there are no reliable structural data available for portlandite below the phase transition. As expected, the average O–H distance increases slightly to a value of 0.99 Å. This together with the strengthening of the hydrogen bond leads to a symmetrization of the O–H···O bond. In accordance with the theory of 'internal' pressure the structure of Sr(OD)$_2$ [24] at ambient conditions bears some similarities to Ca(OH)$_2$-II. Like Ca(OH)$_2$-II, it consists of 7-coordinated AO$_7$ polyhedra forming a three-dimensional network through shared edges, where the hydrogen/deuterium atoms are situated in the cavities within this structure (Fig. 3). The O–H···O bonding has bond lengths around 1.03 Å and 1.9 Å, respectively and O–H···O angles of 155°. These values are similar to those found for Ca(OH)$_2$-II. High pressure investigations on Sr(OH)$_2$ are under way. In view of the similarities between Sr(OH)$_2$ and Ca(OH)$_2$-II, it is fair to assume that a notion of how Sr(OH)$_2$ might behave at high pressure can be obtained by looking at the crystal chemistry of Ba(OH)$_2$. Ba(OH)$_2$ shows even higher coordination numbers for the metal cation (7- and 8-fold). In addition, there exist two phases with distinct crystal structures, separated by only a moderate energy barrier. The monoclinic ($P2_1/n$) β-phase, stable at room temperature (RT), undergoes a phase transition to the orthorhombic ($Pnma$) α-phase at 526(1) K. The high-temperature (HT) phase is quenchable to RT where it is stable in the absence of humidity. The hydrogen bonding in the β-phase is quite similar to the one in the Ca(OH)$_2$-II and Sr(OD)$_2$ with average values of 0.98 Å, 2.07 Å and 163 ° for the O–H, O···H and O–H···O distances and angle, respectively. As expected for a structure stabilized at high temperature, the O–H···O bonds in the HT α-phase show a pattern characteristic for weaker hydrogen bonding with average values of 0.92 Å, 2.73 Å and 136°, respectively. Furthermore, four out of six hydrogen positions in the α-phase exhibit bi- or trifurcated hydrogen bonds. High-pressure studies on Ba(OH)$_2$ are not trivial mainly due to the material's sensitivity to water and CO$_2$, making the loading of a diamond anvil cell with this material a challenge. We nevertheless succeeded in performing a powder X-ray diffraction experiment on β-Ba(OH)$_2$. The experiment reveals at least one phase transition for the β-phase, which again involves an increase in coordination number from 8 to

9 [25]. Not too surprising, this phase is different from the high-pressure form of BaF$_2$, which adopts the cotunnite-type structure at 3 GPa [26]. Hydrogen positions could not be determined from the powder X-ray experiment. A pressure dependent neutron experiment has not been performed as yet. However, the deuterium positions of α- and β-Ba(OH)$_2$ could be followed with neutron diffraction down to 20 K. As in other examples [27], this experiment demonstrated that the volume reducing effect of very low temperature has quite different structural consequences from a volume constraint caused by high-pressure. β-Ba(OH)$_2$ did not show any phase change at all down to 20 K, while the α-phase showed a phase transition which in its structural mechanism is quite similar as it has been observed for brucite at moderate pressures [28]. The origin of this phase transition between 100 K and 150 K is an ordering of one of the deuterium positions, which at higher temperatures displayed a dynamic disorder across a mirror plane. The collective freezing-in on one position of this deuterium atom causes a symmetry reduction from $Pnma$ to $P2_1/n$ [28]. This behavior can thus be compared to the postulated freezing-in phase transition of brucite around 11 GPa [18].

In summary, the available structural data on A(OH)$_2$ allow some conclusions with respect to the behavior of hydrogen bonds as a function of pressure and chemistry: Hydrogen bonds, as weak as they are, have a decisive influence on the lattice energy. This is evidenced by the effect they have on the crystal structure of a given compound, when OH$^-$ is replacing F$^-$ as monovalent anion. As described above, MgF$_2$ (rutile structure), CaF$_2$, SrF$_2$ and BaF$_2$ (fluorite structure) have completely different structures compared to their hydroxyl equivalents. However, when it comes to the reaction of a structure at high pressure, hydrogen bonds seem to act more passively by adapting according to the needs of the valence requirements of the framework atoms, rather than being the driving forces behind such phase transitions. Based on our experiments and data from the literature we propose that the strengths of hydrogen bonds are determined by the coordination number and network topology of the framework rather than by external pressure. Based on this we postulate that phase transitions in hydrous compounds are controlled by the changing ratio of ionic radii between anion and cations, rather than instabilities of the weakly bonded (OH)$^-$ units. The pres-

ence of hydrogens in the structure, however, gives additional flexibility with respect to volume optimization, since the symmetrization of O–H···O bonds allows for stress relaxation, also for the non-hydrogen atoms through a redistribution of the electrons in the crystal structure [29][30]. An explanation for this can be given in the framework of the bond-valence model [30]. For a given stoichiometry (A(OH)$_2$ in this case) with atoms of a given atomic valence (formal charge, 2+ and 2– for the framework atoms in this case), the flexible hydrogen bond can adapt its geometry easily in order to balance valence-sum requirements of the framework atoms, which are mainly controlled by coordination numbers and bond lengths [30]. These factors, in turn, are mainly determined by the relative effective ionic radii of the ions and the polymerization of the structural units. We justify our hypotheses by the following observations:

– The hypothesis that the strength of the hydrogen bonding is determined by the topology of the framework is supported by the observation that both Sr(OD)$_2$ and Ca(OH)$_2$-II, show very similar strengths of the hydrogen bonds, although the Sr compound is measured at ambient conditions, while the Ca-bonding has been calculated from data recorded at high pressure. Thus, the strength of a hydrogen bond is not determined by the external pressure, but rather by the coordination numbers and polymerization of the framework atoms.

– The similarity between the structures of Ca(OH)$_2$-II at high pressure and Sr(OH)$_2$ at ambient conditions suggests that it is not the weak hydrogen-bonds, which drive the pressure-induced phase transition in Ca(OH)$_2$, but rather the pressure-induced increase of the ratio between cation and anion radii. Thus, apart from minor structural modifications such as hydrogen ordering (as seen in brucite at high pressure and α-Ba(OH)$_2$ at low temperature) it is mainly the relative effective size of the framework cations and anions, which controls the structural behavior of hydroxides in P-T space.

– The fact that the hydrogen bonding in Ca(OH)$_2$-II is quite strong and not at all relaxed, although it had been measured very close to the phase transition, gives support to the notion that it is not the stress on the hydrogen bonds, which drives the structural change.

We conclude that hydroxyl groups in inorganic solids do not represent a weak link with respect to compression. From a crystal chemical point of view there is therefore no indication that high pressure expels hydrogen out of a crystal structure. Studies at simultaneously high pressure and high temperature [27] suggest that the effect of pressure on the volume and structure of a material is much more prominent than the effect of temperature. This lets us assume that this finding would also hold at conditions of combined high pressure and high temperature. Crystal chemically it is therefore conceivable that hydrogen can be transported from the surface to the lower mantle along subduction zones e.g. in some sort of hydrous magnesium silicates [31].

4. From Minerals to Modern Materials

Light is used routinely as a carrier to transmit information around the globe. The processing and storage of information, however, still relies largely on electronic and magnetic devices. The introduction of electro-optical devices in this domain promises important progress. Higher speed, larger bandwidth and an increase in storage density by several orders of magnitude are the most important assets of this technology. In order for electro-optic devices to replace current electronic parts, appropriate materials with specific optic properties are needed. Inorganic non-linear optical materials have a potential advantage over organic analogs due to their higher expected mechanical and chemical stability. A focused search for such material is thus highly desirable. Nevertheless, the search for novel inorganic material exhibiting the desired optical properties relies largely on a cook and look procedure. A more directed approach, aiming at understanding the fundamental relationship between crystal chemistry and crystal physics, could – if successful – help to find inorganic material with specific optical properties much easier. In the quest to attain this goal, the study of mineral structures is helpful. The chemical and structural variability of minerals allows to disclose crucial relationships between crystal chemistry and crystal physics.

Many of the non-linear optical materials which are commercially used, contain octahedrally coordinated d^0-transition metals (e.g. $KTiOPO_4$, $LiNbO_3$, $KNbO_3$). The reason for this lies in the intrinsic tendency for such structural units to undergo an electronically induced structural distortion [32][33]. This distortion is characterized by a shift of the d^0 transition metal out of the center of its octahedral coordination polyhedron (out-of-center distortion). The extent to which this distortion is expressed depends on the molecular overlap between metal cation and oxygen anion [32]. Orbital overlap, in turn, can be modified by varying cation size and ionic charge [34]. Out-of-center distortions in MO_6 octahedra cause an electronic hyperpolarizability within the structure which, if embedded in a non-centrosymmetric arrangement, leads to the desired non-linear optical properties. Whether or not a structure containing this cooperatively distorted MO_6 octahedra exhibits a centro-symmetric structure depends heavily on the mutual orientation of the distortion vectors themselves, i.e. the mutual interaction between the distortion vectors. Looking at various $ABOCO_4$-type structures, one finds that the out-of-center distortions of the TiO_6 units are all in parallel e.g. for $KTiOPO_6$ (KTP), which in turn is a well-known non-linear optical material. The mineral titanite, $CaTiOSiO_4$, in contrast, although topologically very similar to KTP, has its distortion vectors parallel within one extended octahedral chain, but anti-parallel between neighboring chains. This leads to a cancellation of the desired hyperpolarizability in titanite. As a consequence, titanite does not show any technically interesting optical properties, although all necessary ingredients (extended chains of corner-linked, distorted TiO_6 octahedra) are present. It is fair to assume that this different behavior in KTP and titanite is somewhat based in the connectivity of the structural units. This hypothesis is confirmed by the following observation: Among the family of $ABOCO_4$ type structures, there is a series of structure types (e.g. $KTiOPO_4$, $K(Mg_{1/3}Nb_{2/3})OPO_4$, γ-$NaTiOPO_4$), which all show more or less parallel orientation of the distortion vector. Interestingly, these structure types can all be deduced through different ordering schemes from one disordered type ($Cs(Ti,As)PO_5$; CTP), where octahedra and tetrahedra are randomly disordered on one framework position [35]. The titanite structure type differs from the CTP type in that neighboring corner-
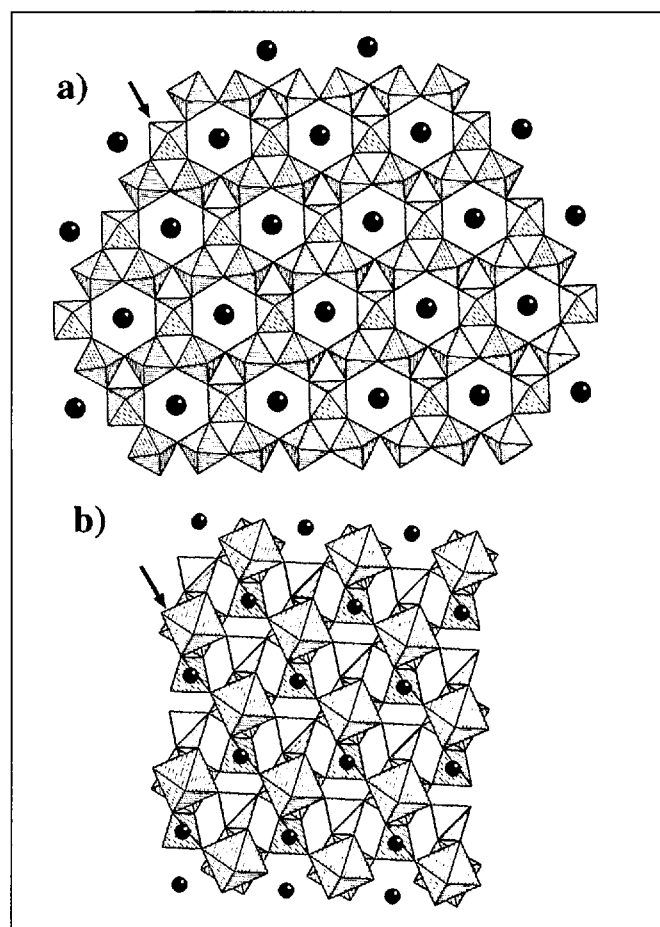

Fig. 4. Comparison of the structures of a) $CsTiOPO_4$ and b) $CaTiOSiO_4$. The octahedra in a) represent positions randomly occupied by TiO_6 octahedra and PO_4 tetrahedra (see [35]). The arrows highlight corresponding ...cis... cis.... octahedral chains found in titanite-type structures (extended perpendicular to the projection). Note that the mutual connection of these chains is different in a) and b) (see text).

linked *trans-trans* chains of octahedra are mutually linked through one ortho-group instead of two as in CTP. For this reason, the CTP network cannot be transformed into the titanite structure type by any conceivable ordering scheme (Fig. 4).

The mechanism how the topology, *i.e.* polyhedral connectivity couples with the ordering scheme of the distortion vectors is unknown so far. Possible clues on the coupling of the distortion vectors can be gained by understanding the various phase transitions found in titanite-type structures and KTP structures. Our efforts concentrated so far on titanite-type compounds such as titanite ($CaTiOSiO_4$) and malayaite ($CaSnOSiO_4$). These two compounds are of particular interest to compare, since they are topologically identical. However, titanite, having Ti in the octahedral position, displays the expected out-of-center distortion, while malayaite, where the d^0-transition metal Ti^{4+} is replaced by the main-group element Sn^{4+}, has a regular octahedral surrounding.

At ambient conditions, $CaTiOSiO_4$ crystallizes in space-group $P2_1/a$. Titanite is known to exhibit a series of T- and P-driven phase transitions, which are all linked to either order/disorder or suppression of the characteristic out-of-center distortion of the Ti^{4+}. At around 500 K, a first transition is mainly controlled by an order–disorder process between distortion vectors [36]. This phase transition is characterized by a change of symmetry from $P2_1/a$ to $A2/a$. As shown through the study of diffuse intensity in the vicinity of symmetry forbidden reflections [37], the disordering occurs between adjacent octahedral chains, while all octahedra within a chain remain distorted in a cooperative way. The diffuse intensity decreases with increasing temperature until it completely disappears around 825 K [38]. At this temperature, an isosymmetric ($A2/a$ <-> $A2/a$) phase-transition occurs. This phase transition is linked to the Ti-bonding as evidenced by a collapse of the IR Ti–O stretching mode at the transition temperature [39]. This behavior is interpreted as the disappearance of the out-of-center distortion also on a local scale. The Ti potential changes from a two-well potential into a flat single well.

The interpretation of the 825 K transition as a disappearance of the out-of-center distortion is corroborated by a high-pressure phase transition at ~ 3.5 GPa [40]. Again this phase transition shows a change of symmetry from $P2_1/a$ to $A2/a$. Based on crystal-chemical arguments, it is shown that this symmetry change is caused by a true symmetrization of the TiO_6 octahedra rather than by a disorder process. When following the pressure-induced phase transition as a function of temperature, one finds that the transition pressure decreases with increasing temperature [27]. The negative slope of the phase boundary extrapolates to ~ 850 K at zero pressure. This therefore links the high-pressure phase transition at 3.5 GPa with the high-temperature phase transition at 825 K.

It is not clear at this stage to what extent the electronically induced distortion on one hand and topological effects on the other hand are controlling these various phase changes. In order to be able to clearly separate the two effects, a comparison with an iso-structural analog without d^0-transition metal is most useful. The most suitable material for such a comparison is malayaite ($CaSnOSiO_4$). This mineral is iso-structural to titanite with Ti^{4+} replaced by Sn^{4+}. Ti^{4+} and Sn^{4+} in octahedral coordination have very similar radii (0.69 Å and 0.61 Å respectively) and identical charge. They differ by their electronic configuration, Sn^{4+} being a main group element and Ti^{4+} a d^0 transition metal. As expected malayaite does not express any structural distortions at the SnO_6 octahedra. It therefore crystallizes in the aristotype space group $A2/a$ at ambient conditions. It is interesting to note that the stepwise substitution of Ti^{4+} with Sn^{4+} in titanite leads to space group $A2/a$ already at a Sn/Ti ratio lower than 0.1 [41]. This suggests an only weak coupling between the distortion vectors. When malayaite is subject to high temperature, no structural phase transition could be detected so far. Zhang *et al.* [42]
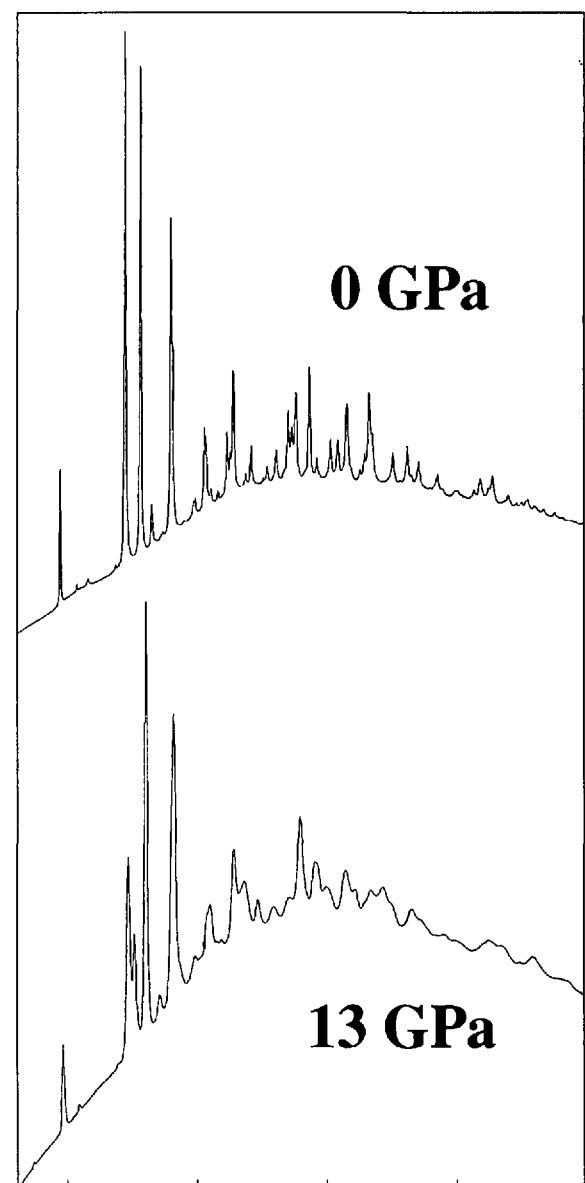

Fig. 5. The powder pattern of $CaTiOSiO_4$ changes drastically above ~ 9 GPa. The high-pressure pattern could not be indexed so far. It is possible that the new pattern evidences a similar phase as found in malayaite above 5 GPa (see text).

observed a discontinuity in the temperature evolution of the phonon frequency and IR absorbance near 500 K. However, they were not able to correlate this with any symmetry breaking structural change or split positions. A more surprising result is found when compressing malayaite to 5 GPa. Here the symmetry of the crystal structure is reduced from monoclinic $A2/a$ to triclinic $P1$ [43]. The phase transition is characterized by a rigid-body tilting of the SnO_6 octahedra. This leads to two symmetrically distinct octahedral chains. The tetrahedra follow this rigid movement by an internal distortion similar to that observed in $A2/a$ titanite upon compression [27]. As a response on the imposed volume constraint the Ca atoms move parallel [101]. This brings them closer to an eighth oxygen atom (bond valence increases from ~0.05 v.u. to 0.1 v.u.). Whether or not this symmetry breaking phase transition is preceded by an iso-symmetric phase transition around 3 GPa is the matter of current investigation.

The absence of any phase change in malayaite at high temperature is in accordance with the hypothesis that the structural transitions in titanite are only controlled by the electronically induced distortions. The fact that the phase transition at high pressure is completely different from the one observed in titanite further corroborates this notion. Although titanite and malayaite have the same structural topology, such a symmetry-reducing phase transition has not conclusively been seen for titanite as yet. We did observe a clear and reproducible change of a powder diffraction pattern for titanite at pressures around 10 GPa (Fig. 5). Unfortunately we were not able to index this pattern and thus were not able to prove that this change is due to a symmetry reduction or merely an effect of the pressure medium becoming non-hydrostatic [8]. The appearance of new peaks is likely to be a real effect. The fact that we do not manage to index the new powder pattern, however, could be related to deviatoric stress within the pressure chamber.

In view of the relatively easy way to manipulate the expression and mutual correlation of the out-of-center distortion, it is conceivable that it might be possible to force these distortions into a parallel arrangement. This could be attempted, for example, by heating the material above the order–disorder temperature of 500 K and then cooling it down in the presence of a strong directed electric field. If this is successful, titanite could be converted from a 'mere' rock-forming mineral into an interesting non-linear optical material.

[1] R.M. Hazen, L.W. Finger, 'Comparative Crystal Chemistry', John Wiley & Sons, New York, 1982; L. Merrill, W.A. Bassett, *Rev. Sci. Instrum.* 1974, 45, 290; J.M. Bassett, L.C. Ming, *Phys. Earth Plan. Mat.* 1972, 6, 154.

[2] O. Shimomura, K. Takemura, H. Fujihisa, Y. Fuji, T. Ohishi, T. Kikegawa, Y. Amemiya, T. Matsushita, *Rev. Sci. Instrum.* 1992, 63, 967.

[3] M. Thoms, S. Bauchau, D. Häusermann, M. Kunz, T. LeBihan, M. Mezouar, D. Strawbridge, *Nuc. Instrum. Meth. Phys. Res.* 1998 A 413, 175.

[4] A.P. Hammersley, S.O. Svensson, A. Thompson, H. Graafsma, Å. Kvick, J.P. Moy, *Rev. Sci. Instrum.* 1995, 66, 2729.

[5] D. Andrault, G. Fiquet, M. Kunz, F. Visocekas, D. Häusermann, *Science* 1997, 278, 831–834; G. Fiquet, A. Dewaele, D. Andrault, M. Kunz, T. LeBihan, *Geophys. Res. Let.* 2000, 27(1), 21–24.

[6] A. Van Valkenburg, *Diamond Research* 1964, 17; C.E. Weir, S. Block, G. Piermarini, *J. Res. Nat. Bur. Stand.* 1965, C 69, 275.

[7] A. Jayaraman, *Rev. Mod. Phys.* 1983, 55, 65; A.P. Jephcoat H.K. Mao, P.M. Bell, in 'Hydrothermal Experimental Techniques', Eds. G.C. Ulmer, H.L. Barnes, John Wiley, New York, 1987, 469; D.J. Dunstan, I.L. Spain, *J. Phys. E, Scientific Instruments* 1989, 22, 913; I.L. Spain, D.J. Dunstan, *J. Phys. E, Scientific Instruments* 1989, 22, 923; M.I. Eremets 'High Pressure Experimental Methods', Oxford University Press, Oxford New York Tokyo, 1996.

[8] R. Miletich, D.R. Allen, W.F. Kuhs, in 'Reviews in Mineralogy and Geochemistry', Ed. R.M. Hazen, Mineralogical Society of America, Washington D.C., 2001, 41, 445.

[9] D.R. Allan, R. Miletich, R.J. Angel, *Rev. Sci. Instrum.* 1996, 67, 840.

[10] R. Miletich, H. Reifler, M. Kunz, *Acta Cryst.* 1999, A55, Suppl., P08.CC.001

[11] R. Boehler, M. Nicol, M.L. Johnson, in 'High Pressure Research in Mineral Physics', Ed. M.H. Manghnani, Y. Syono, 1987, 173; R. Boehler, M. Nicol, C.S. Zha, M.L. Jonson, *Physica B* 1986, 139, 916.

[12] R.J. Hemley, P.M. Bell, H.K. Mao, *Science* 1987, 237, 605.

[13] M.S. Weathers, W.A. Bassett, *Phys. Chem. Min.* 1987, 15, 105.

[14] W.A. Bassett, M.S. Weathers, in 'High-pressure Research in Mineral Physics', Ed. M.H. Maghnani, Y. Syono, 1987, 129.

[15] A.B. Thompson, *Nature* 1992, 358, 295; J.R. Smyth, *Amer. Mineral.* 1994, 79, 1021.

[16] A.E. Ringwood, A. Major, *Earth Planet. Sci. Lett.* 1967, 2, 106.

[17] J.B. Parise, K. Leinenweber, D.J. Weidner, K. Tan, R.B. Von Dreele, *Amer. Mineral.* 1994, 79, 193.

[18] M. Catti, G. Ferraris, S. Hull, A. Pavese, *Phys. Chem. Mineral.* 1995, 22, 200.

[19] T.S. Duffy, *EOS, Spring Meeting, Abs.* 1993 m42B-8, p169.

[20] L. Desgranges, D. Grebille, G. Calvarin, G. Chevrier, N. Floquet, J.C. Niepce, *Acta Cryst.* 1993, B49, 812.

[21] C. Meade, R. Jeanloz, *Geophys. Res. Lett.* 1990, 117(8), 1157; M. Kunz, D.J. Weidner, M. Vaughan, J.B. Parise, Y. Wang, K. Leinenweber, *NSLS Activity Report Abstracts* 1994 Abstract-#: KUX17384C.

[22] K. Leinenweber, *National Synchrotron Light Source, Annual Report* 1993.

[23] M. Kunz, K. Leinenweber, J.B. Parise, T.-C. Wu, W.A. Bassett, K. Brister, D.J. Weidner, M. Vaughan, Y. Wang, *High Press. Res.* 1996, 14, 311.

[24] D.E. Partin, M. O'Keeffe, *J. Solid St. Chem.* 1995, 119, 157.

[25] A. Friedrich, M. Kunz, R. Miletich, 2001, in preparation

[26] J.M. Leger, J. Haines, A. Atouf, O. Schulte, *Phys. Rev. B* 1995, 52(18), 13247.

[27] M. Kunz, T. Arlt, J. Stolz, *Amer. Mineral.* 2000, 85, 1465.

[28] A. Friedrich, M. Kunz, E. Suard, 2001, in preparation.

[29] F.C. Hawthorne, in 'The Stability of Minerals', Eds. G.D. Price, N.L. Ross, Chapmann & Hall, London, 1992, p25.

[30] I.D. Brown, *Acta Cryst.* 1992, B48, 553.

[31] R. Van der Voo, W. Spakman, H. Bijwaard, *Nature* 1999, 397, 246; P. Ulmer, V. Trommsdorff, *Science* 1995, 268, 858.

[32] J.K. Burdett, 'Molecular Shapes', Wiley Interscience, New York, 1980.

[33] M. Munowitz, R.H. Jarman, J.F. Harrison, *Chem. Mat.* 1993, 5, 661.

[34] M. Kunz, I.D. Brown, *J. Solid St. Chem.* 1995, 115, 395.

[35] M. Kunz, R. Dinnebier, L.K. Cheng, E.M. McCarron III, D.E. Cox, J.B. Parise, M. Gehrke, J. Calabrese, P.W. Stephens, T. Vogt, R. Papoular, *J. Solid St. Chem.* 1995, 120, 299.

[36] M. Zhang, E.K.H. Salje, U. Bismayer, H. Unruh, B Wruck, C. Schmidt, *Phys. Chem. Miner.* 1995, 22, 41.

[37] T. Malcherek, C. Paulmann, U. Bismayer, *Eur. J. Mineral.* 2000, Beiheft 1, 118.

[38] S. Kek, M. Aroyo, U. Bismayer, C. Schmidt, K. Eichhorn, H.G. Krane, Z. *Krist.* 1997, 212, 9.

[39] M. Zhang, E.K.H. Salje, U. Bismayer, *Amer. Mineral.* 1997, 82, 30.

[40] M. Kunz, D. Xirouchakis, D.H. Lindlsey, D. Häusermann, *Amer. Mineral.* 1996, 81, 1527; R.J. Angel, M. Kunz, R. Miletich, A.B. Woodland, R. Koch, D. Xirouchakis, *Phase Trans.* 1999, 68, 533.

[41] M. Kunz, D. Xirouchakis, Y. Wang, J.B. Parise, D.H. Lindsley, *Schweizerische Mineral. Petrogr. Mitt.* 1997, 77, 1.

[42] M. Zhang, H.-W. Meyer, L.A. Groat, U. Bismayer, E.K.H. Salje, G. Adiwidjaja, *Phys. Chem. Miner.* 1999, 26, 546.

[43] S. Rath, M. Kunz, R. Miletich, 2001, in preparation.